

## Degradation kinetics and mechanisms of phenol in photo-Fenton process\*

HE Feng (何 锋), LEI Le-cheng (雷乐成)<sup>†</sup>

(Department of Environmental Engineering, Zhejiang University, Hangzhou 310027, China)

<sup>†</sup>E-mail: lclei@mail.hz.zj.cn

Received Feb. 10, 2003; revision accepted May 20, 2003

**Abstract:** Phenol degradation in photochemically enhanced Fenton process was investigated in this work. UV-VIS spectra of phenol degradation showed the difference between photo-Fenton process and UV/H<sub>2</sub>O<sub>2</sub>, which is a typical hydroxyl radical process. A possible pathway diagram for phenol degradation in photo-Fenton process was proposed, and a mathematical model for chemical oxygen demand (COD) removal was developed. Operating parameters such as dosage of H<sub>2</sub>O<sub>2</sub> and ferrous ions, pH, suitable carrier gas were found to impact the removal of COD significantly. The results and analysis of kinetic parameters calculated from the kinetic model showed that complex degradation of phenol was the main pathway for removal of COD; while hydroxyl radicals acted weakly in the photo-Fenton degradation of phenol.

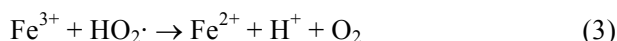
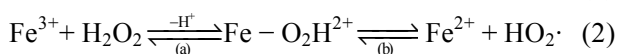
**Key words:** Phenol, Photo-Fenton process, Kinetics, Radical oxidation, Complex oxidation

**Document code:** A

**CLC number:** TQ150.9; X783

### INTRODUCTION

Fenton process has been well studied recently for its prospective applications in unmanageable wastewater treatment (Legrini *et al.*, 1993; Ollis and Al-Ekabi, 1993; Prousek, 1996). The high efficiency of this process is traditionally thought to be due to the generation of hydroxyl radical (HO·), which is of a high oxidation potential ( $E^0 = 2.80$  V) and can mineralize the organic compounds completely to water and carbon dioxide. In acidic medium, this radical mechanism can be simply described by the following equations (Walling, 1975):



The combination of Fenton reaction in UV (Ultraviolet) light, the so-called photo-Fenton reaction, had been shown to enhance the efficiency of the Fenton process. Some researchers also attributed this to the decomposition of the photo-active  $\text{Fe}(\text{OH})^{2+}$  which lead to the addition of the HO· radicals (Sun and Pignatello, 1993).



However, the free radical mechanism had been questioned at times (Walling and Amarnath, 1982; Kremer, 1985). The alternative mechanisms maintained that complexes and compounds between Fe(III) and H<sub>2</sub>O<sub>2</sub> are the actual intermediates in the reaction. Optical absorption measurements during the reaction also proved the presence of these complexes (Kremer and Stein, 1959). Recently, Bossmann's work on advanced oxidation of PVA using

\* Project (No. 20176053) supported by the National Natural Science Foundation of China

using photo-Fenton process yielded experimental evidence for the formation of supermolecule from Fe(III)/(II)-PVA and no low molecular weight intermediates were detected during the PVA-degradation. The Fenton-type oxidation of PVA proceeded via a ferrylion (+IV) formed by a two-electron inner-sphere electron transfer reaction within the complex PVA/Fe<sup>2+</sup> and CO<sub>2</sub> was released directly from the super-macromolecule (Bossmann *et al.*, 1998; 2001; Lei *et al.*, 1998).

Spin-trapping experiments showed that free hydroxyl radicals exist in Fenton or photo-Fenton reactions (Jiang *et al.*, 1993). After study of relevant literature, we consider that hydroxyl radical oxidation and/or some other complex reaction occur in the photo-Fenton process. The problem is that hydroxyl radicals can oxidize simple organic pollutants directly, while refractory ones such as PVA can only be degraded through complex pathway.

The kinetics of pollutant degradation in Fenton or Photo-Fenton process in the hydroxyl radical reaction mechanism had been well established by many researchers (Gallard and Laet, 2000; Andreozzi *et al.*, 2000). However, kinetics studies which include both HO· reaction and complex oxidation in photo-Fenton process, have rarely been reported. This work, with phenol chosen as the model organic compound established the kinetic model, wherein HO· reaction pathway or some other complex pathway are involved in the photo-Fenton process; one way is through the inner-sphere electron transfer where phenol directly oxidized to CO<sub>2</sub> and H<sub>2</sub>O; in the other way, phenol is first converted to organic acid under the attack of HO·, then oxidized to CO<sub>2</sub> and H<sub>2</sub>O. Operating parameters such as H<sub>2</sub>O<sub>2</sub> variation, Fe<sup>2+</sup> variation, initial pH, purge-gas were studied to investigate the validity and feasibility of the proposed model.

## EXPERIMENTAL SECTION

### Materials

FeSO<sub>4</sub>·7H<sub>2</sub>O, FeCl<sub>3</sub>·6H<sub>2</sub>O, H<sub>2</sub>O<sub>2</sub>, H<sub>2</sub>SO<sub>4</sub>, NaOH, phenol, 1,10-phenanthroline acetonitrile and acetic acid were all analytical grade, catalase was purchased from Worthington; water was of double-

distilled quality. All other chemicals were ACS grade.

### Photoreactor and photodegradation procedure

All photolysis experiments were carried out in a batch reactor. Fig.1 shows the experimental setup consisting of a reservoir (*V*=1.00 L), a flow-through annular photoreactor (*V*=0.30 L) equipped with a mercury medium pressure lamp (Philips, GGZ 300) and a quartz filter. The solution was recirculated (250 ml/min) by a pump (Masterflex). The phenol solution was continuously purged (in the reservoir) by O<sub>2</sub> during the entire reaction time. All photolysis experiments were performed for 60 min. The temperature of the solutions was kept at 30 °C.

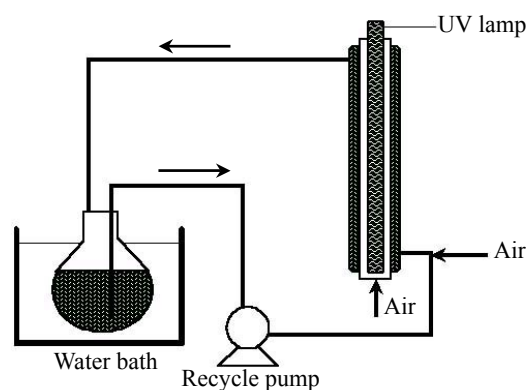
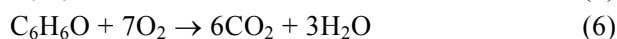
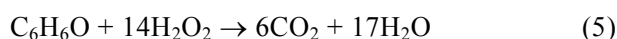


**Fig.1** Photochemical batch reactor employed in all irradiation experiments

The total volume of the photolysis solution was 1.00 L. The initial concentration of the phenol solution was 100 mg/L. FeSO<sub>4</sub>·7H<sub>2</sub>O was added into the phenol solution before H<sub>2</sub>O<sub>2</sub> was added. The stoichiometric amount of H<sub>2</sub>O<sub>2</sub> (*Q*<sub>th</sub>) required for the total oxidation of phenol was calculated by using Eq.(5).



The pH was adjusted by using proper H<sub>2</sub>SO<sub>4</sub>. Oxidation was monitored by measurement of chemical oxygen demand (COD). Residual H<sub>2</sub>O<sub>2</sub> was consumed by enzyme catalase to prevent interference with COD analysis.

### Analytical methods

UV/VIS (8500 spectrophotometer, Techcomp) was used to measure the UV-VIS spectra of the phenol solutions, while pH was measured by Rex-pH-analyzer (PHS-25).

COD analysis was carried out by titrimetric method. Analysis of ferrous irons was conducted by using the modified 1,10-phenanthroline colorimetric method at 510 nm.

## RESULTS AND DISCUSSIONS

### Comparison of UV/VIS-Absorption Spectra during photo-Fenton and UV/H<sub>2</sub>O<sub>2</sub> phenol degradation

UV/VIS spectra of the reaction mixture during the UV/H<sub>2</sub>O<sub>2</sub> and photo-Fenton degradation of phenol are shown in Fig.2 and Fig.3, respectively. As UV/H<sub>2</sub>O<sub>2</sub> process is a typical hydroxyl radical reaction, its spectra change in phenol degradation was investigated for comparison with that of photo-Fenton process. Fig.2 shows that addition of H<sub>2</sub>O<sub>2</sub> in phenol solution does not change the spectral character peak of the reaction solution. No complex with high absorbance was formed in this process. Light absorption at phenol's absorption peaks (209 nm, 269 nm) decreases evenly with time. Moreover, a new peak (320 nm, though not very obvious) appears at 10 min in the spectra. These spectra results indicate the degradation of the phenol and the forma-

tion of intermediates with characterizing absorption at 320 nm. At 20 min, the character peaks (209 nm, 269 nm) of phenol disappears and its absorption at 320 nm also decreases. So all phenol have been oxidized at this time and the formed intermediates are being further oxidized to CO<sub>2</sub> and H<sub>2</sub>O.

Fig.3 shows the UV/VIS absorption spectra occurring during photochemically enhanced Fenton degradation of phenol. It is noteworthy that a colloid with high absorption at 200 nm to 400 nm formed at the moment of FeSO<sub>4</sub>·7H<sub>2</sub>O addition to phenol and H<sub>2</sub>O<sub>2</sub> mixture. At the same time phenol's characterizing peaks disappear in the UV/VIS spectra. Fig.4 and Fig.5 show that no complex with high absorbance can be formed between Fe(III)/Fe(II) and phenol under the irradiation. Iron may appear in a new valence state (as Fe(+IV) or Fe(+V)) in the formed complex (colloid). With reaction going on, no new absorption peak could be found in the photo-Fenton process spectra. Some phenol was degraded through the inner electron transfer in photo-Fenton process. This observation is greatly different from the degradation of phenol in UV/H<sub>2</sub>O<sub>2</sub> process. Both complex and low molecular weight intermediates should be generated in photo-Fenton degradation of phenol, wherein photolysis of H<sub>2</sub>O<sub>2</sub> also occurs.

### Kinetic model

The UV/VIS spectra of phenol degradation in

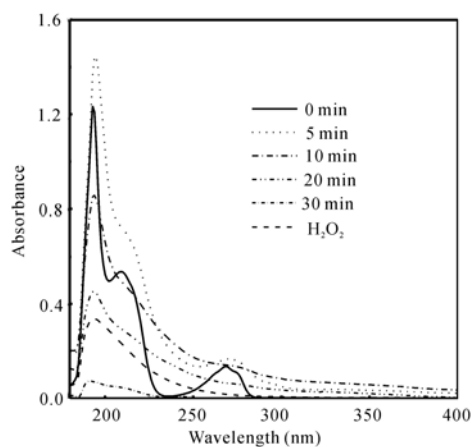


**Fig.2 UV-spectra during the UV/H<sub>2</sub>O<sub>2</sub> reaction in the presence of phenol**

Operational conditions: H<sub>2</sub>O<sub>2</sub> Q<sub>th</sub>, temperature 30 °C, pH 3

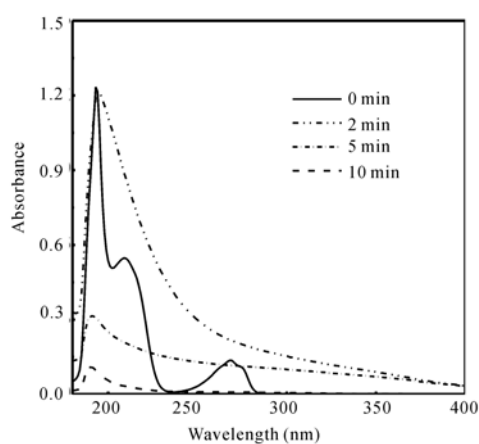


**Fig.3 UV-spectra during the photo-Fenton reaction in the presence of phenol**

Operational conditions: H<sub>2</sub>O<sub>2</sub> Q<sub>th</sub>, FeSO<sub>4</sub>·7H<sub>2</sub>O 207 mg/L, temperature 30 °C, pH 3

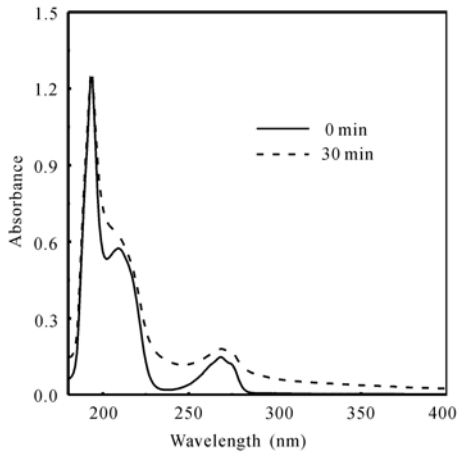


**Fig.4 UV-spectra during the photolysis of phenol and ferric ion solution**

Operational conditions:  $\text{FeSO}_4 \cdot 7\text{H}_2\text{O}$  207 mg/L, temperature 30 °C, pH 3

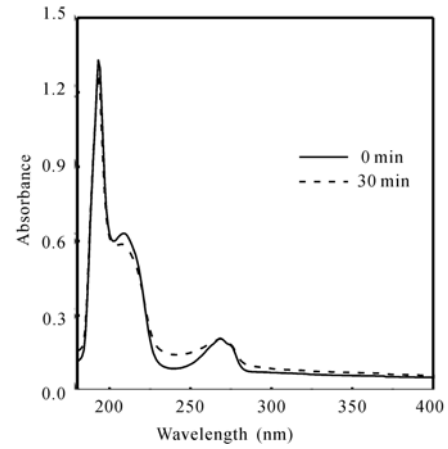


**Fig.5 UV-spectra during the photolysis of phenol and ferric ion solution**

Operational conditions:  $\text{FeCl}_3 \cdot 6\text{H}_2\text{O}$  201 mg/L, temperature 30 °C, pH 3

UV/ $\text{H}_2\text{O}_2$  and of photo-Fenton process shows that phenol degradation can probably proceed through two pathways: complex oxidation and  $\text{HO}\cdot$  oxidation. Fig.6 may represent the principal pathways of phenol degradation.

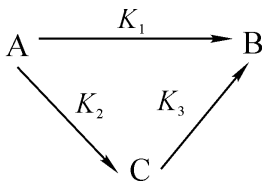


**Fig.6 The principal pathways of phenol degradation**

In the above reaction pathways (Fig.6), A represents the original organic compound (phenol), B is the organic intermediates such as acetic acid, etc., and C is the final substrates,  $\text{CO}_2$  and  $\text{H}_2\text{O}$ .  $K_i$  ( $i = 1, 2, 3$ ) is the apparent rate constant ( $\text{min}^{-1}$ ). The pathway from A to C represents the complex reaction; that from A to B to C represents the radical reaction.

If all reactions can be simplified to pseudo-first-order kinetics, the following set of differential equations could be obtained according to the reaction diagram:

$$-\frac{d[A]}{dt} = (K_1 + K_2)[A] \quad (7)$$

$$-\frac{d[B]}{dt} = K_3[B] - K_2[A] \quad (8)$$

where  $[A]$  represents the concentration of the phenol,  $[B]$  represents the concentration of the organics except A.

In a homothermal ideal reactor with periodical continuous current, the apparent rate constant  $K_i$  can be written as follows:

$$K_1 = k_1^0 e^{-E_1/RT} \quad (9)$$

$$K_2 = k_2^0 e^{-E_2/RT} \quad (10)$$

$$K_3 = k_3^0 e^{-E_3/RT} \quad (11)$$

$K_i$  is related to reaction parameters such as the dosage of  $\text{H}_2\text{O}_2$  and ferrous ions, pH, suitable carrier gas, and so on.

The integration constants can be evaluated from the initial conditions:

$$\text{At time } t=0, [A]=[A]_0, [B]=[B]_0=0$$

The generalized kinetic model is given by

$$[A] = [A]_0 e^{-(K_1+K_2)t} \quad (12)$$

$$[B] = [B]_0 e^{-K_3 t} + \frac{K_2[A]}{K_1 + K_2 - K_3} [e^{-K_3 t} - e^{-(K_1+K_2)t}] \quad (13)$$

Combining Eq.(12) and Eq.(13) yields:

$$\frac{[A+B]}{[A+B]_0} = \frac{K_2}{K_1+K_2-K_3} e^{-K_3 t} + \frac{K_1-K_3}{K_1+K_2-K_3} e^{-(K_1+K_2)t} \quad (14)$$

$[A+B]$  represents the concentration of all the organic chemicals and,  $[A+B]_0$  is the  $[A+B]$  value at reaction time zero. Applying the kinetic equation to the COD data and with

$$\frac{COD}{COD_0} = \frac{[A+B]}{[A+B]_0} \quad (15)$$

The  $COD-t$  relationship becomes:

$$[COD] = [COD]_0 \left[ \frac{K_2}{K_1+K_2-K_3} e^{-K_3 t} + \frac{K_1-K_3}{K_1+K_2-K_3} e^{-(K_1+K_2)t} \right] \quad (16)$$

This is the equation describing the reduction of COD with reaction time. Moreover, in order to evaluate the proportion of complex reaction to radical reaction, the selectivity  $\alpha$  is defined as  $K_1/K_2$ . The total apparent reaction constant for phenol elimination is defined as  $K=K_1+K_2$ . To explore the feasibility of the model, phenol degradation at different initial concentrations was examined.

#### Effect of initial phenol concentration

Fig.7 shows the effect of initial concentrations of phenol (60 mg/L, 100 mg/L, 200 mg/L) on the evolution of COD. In this figure, the symbols represent the experimental data, while the lines represent the calculated curves fitted by the model that proposed above. Obviously, the curves of COD degradation fitted very well for three initial phenol concentrations (60 mg/L, 100 mg/L, 200 mg/L). The good agreement between the experimental data and the fitted lines of the equation supports well the proposed degradation model of phenol. Calculated kinetics parameters such as  $K_i$  and  $\alpha$  are listed in Table 1.

Table 1 shows that when initial phenol concentration increased from 60 mg/L to 100 mg/L,  $K$

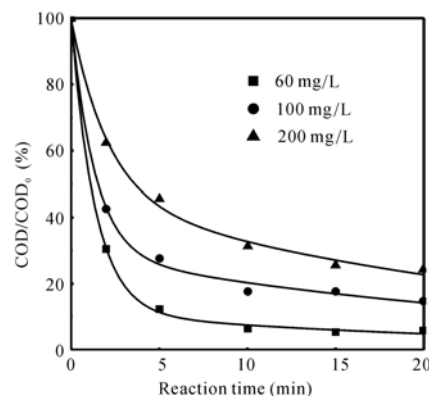


**Fig.7 Phenol solution COD degradation at different initial phenol concentration**

Operational conditions:  $H_2O_2$   $Q_{th}$ ,  $FeSO_4 \cdot 7H_2O$  207 mg/L, temperature 30 °C, pH 3

**Table 1 Calculated results at different initial concentration of phenol**

$[A]_0$ (mg/L)	$K_1$	$K_2$	$K_3$	$K$	$\alpha$
60	0.6630	0.0800	0.0424	0.7430	4.74
100	0.5365	0.2013	0.0349	0.7378	2.67
200	0.2752	0.2030	0.0350	0.4782	1.36

reduced from 0.7430 to 0.7378. However, when the initial phenol concentration increased to 200 mg/L, constant  $K$  sharply reduced to 0.4782. This observation indicates that initial phenol concentration affects the rate of phenol removal insignificantly when it ranged from 60 mg/L to 100 mg/L. The model could be used well to predict degradation of phenol at low concentration.

#### Effect of initial $H_2O_2$ addition

Fig.8 shows the effect of initial addition of  $H_2O_2$  on the COD removal in photo-Fenton degradation of phenol. The reaction constants obtained by nonlinear regression are listed in Table 2. Eq.(16) shows that with sufficiently extended reaction time, the COD approaches zero. That is, given sufficient time, phenol can be completely mineralized to  $CO_2$  and  $H_2O$  in photo-Fenton process.

Table 2 shows that when the  $H_2O_2$  addition is  $1/4 Q_{th}$ , the calculated curve of COD removal deviated from the  $X$ -axis significantly. This can be explained. The rapid exhaustion of the limited  $H_2O_2$  in the initial reaction period leads to the incomplete

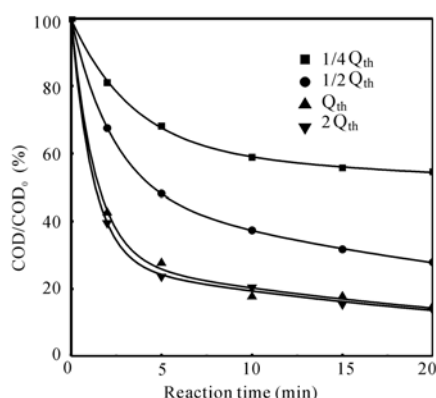


**Fig.8 Effect of initial concentration of  $H_2O_2$  on phenol solution COD degradation**

Operational conditions:  $FeSO_4 \cdot 7H_2O$  207 mg/L, temperature 30 °C, pH 3

**Table 2 Calculated results at different initial concentration of  $H_2O_2$**

$H_2O_2$	$K_1$	$K_2$	$K_3$	$K$	$\alpha$
1/4 $Q_{th}$	0.1202	0.1696	0.0046	0.2898	0.71
1/2 $Q_{th}$	0.2355	0.1936	0.0277	0.4291	1.22
$Q_{th}$	0.5365	0.2013	0.0349	0.7378	2.67
2 $Q_{th}$	0.6116	0.2188	0.0353	0.8304	2.80

oxidation of phenol. When more initial  $H_2O_2$  was added from 1/2  $Q_{th}$  to 2  $Q_{th}$ ,  $K_1$  increased from 0.1202 to 0.6112. However,  $K_2$  kept its value around at 0.2000, from 0.1936 to 0.2188. The increase of  $H_2O_2$  did not lead to a significantly enhanced free radical oxidation of phenol, though better COD removal was achieved with the addition of  $H_2O_2$ . The comparison between  $K_1$  and  $K_2$  shows radical oxidation is not the efficient way for COD removal in photo-Fenton phenol degradation.

Fig.8 shows that when the dosage of  $H_2O_2$  addition is 1/4  $Q_{th}$  and 1/2  $Q_{th}$ , 36.5% and 73.1% COD removal are achieved respectively, which is far more than the assumed rate 25% (1/4  $Q_{th}$ ) and 50% (1/2  $Q_{th}$ ). This phenomenon was mentioned by Weichgrebe and Vogelpohl (1994) and Utset *et al.* (2000). It can be interpreted that dioxygen can serve as the radical acceptor in hydroxyl radical oxidation, so  $O_2$  takes part in the degradation of phenol and leads to the additional removal of COD.

When  $H_2O_2$  ( $Q_{th}$ ) was employed, the experimental results had a plateau region at 85% COD removal

rate. However, this plateau still exists and does not lead to enhanced removal rate of COD when excessively large amount of  $H_2O_2$  (2  $Q_{th}$ ) is employed. This observation suggests that beyond the threshold,  $H_2O_2$  concentration is not the limiting factor of the photo-Fenton process. This observation may be related to the low value of  $K_3$ , which leads to the inefficient removal of residual COD (acetic acid, etc.).

### Effect of $Fe^{2+}$ addition

Fig.9 shows the effect of  $[H_2O_2]/[Fe^{2+}]$  ( $Q=Q_{th}$ ) on phenol degradation. Parameters calculated are listed in Table 3. Similar to the effect of the amount of  $H_2O_2$  added, with increase of iron(II) concentration  $K_1$  increases greatly while  $K_2$  increases slightly. The initial concentration of iron(II) cannot affect the radical oxidation of phenol significantly.

It also can be seen that the value of  $K_3$  is biggest with lowest iron(II) concentration added. Lower iron(II) will consume less  $H_2O_2$  in the initial reaction period. Thus in the process of organic acid oxidation (the period B to C in Fig.6), the residual  $H_2O_2$  plays an active role. Fig.8 shows no significant difference of COD removal for  $[H_2O_2]/[Fe^{2+}]$

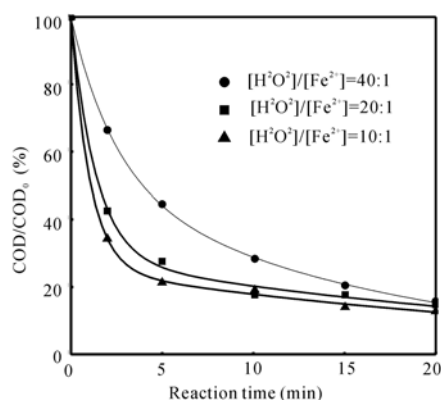


**Fig.9 Effect of initial concentration of ferrous ion on phenol solution COD degradation**

Operational conditions:  $H_2O_2$   $Q_{th}$ , temperature 30 °C, pH 3

**Table 3 Calculated results at different initial concentration of  $Fe^{2+}$**

$[H_2O_2]/[Fe^{2+}]$	$K_1$	$K_2$	$K_3$	$K$	$K_1/K_2$
40:1	0.2326	0.1824	0.0606	0.4150	1.28
20:1	0.5365	0.2013	0.0349	0.7378	2.67
10:1	0.7355	0.2387	0.0353	0.9742	3.08

ratio of 20:1 to 10:1, which means  $[\text{H}_2\text{O}_2]/[\text{Fe}^{2+}] = 20:1$  is preferred.

### Effect of pH

Fig.10 shows the effect of initial pH variation on phenol degradation. Parameters calculated are listed in Table 4.

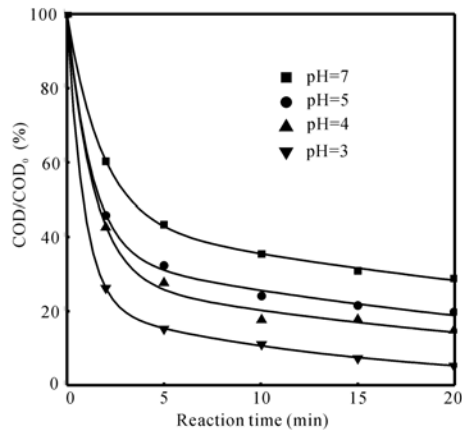


**Fig.10 Effect of initial concentration of pH on phenol solution COD degradation**

Operational conditions:  $\text{H}_2\text{O}_2$   $Q_{\text{th}}$ ,  $\text{FeSO}_4 \cdot 7\text{H}_2\text{O}$  207 mg/L, temperature 30 °C

**Table 4 Calculated results at different Initial concentration of pH**

pH	$K_1$	$K_2$	$K_3$	$K$	$\alpha$
3	0.9337	0.2368	0.0701	1.1705	3.94
4	0.5365	0.2013	0.0349	0.7378	2.67
5	0.5280	0.2654	0.0307	0.7934	1.99
7	0.3215	0.2358	0.0221	0.5573	1.36

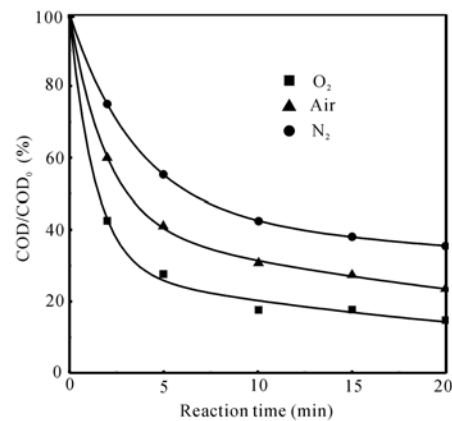
The COD removal rate maximizes at pH 3.0 and it begins to decrease with increase of pH. At pH 7.0, iron(II) cannot keep its active form; the removal rate of COD in both reaction way will decrease. However, since plenty of  $\text{H}_2\text{O}_2$  and UV (Ultraviolet) exist in the photo-Fenton process, the removal of COD can still be achieved at pH=7.

Table 4 shows that  $K_1$  and  $K_3$  are biggest at pH 3.0 among the four pH values and the value of  $\alpha$  ( $>1$ ) decreases with the enhancement of pH. This observation indicates that both complex oxidation of phenol and the further oxidation of organic acid are promoted at low pH. Since pH is a primary effect factor on hydroxyl radical reaction,  $K_2$  will be im-

acted by pH significantly if Fenton reaction is mainly a radical oxidation process. However,  $K_2$  fluctuates slightly with the change of pH and essentially keeps at a constant value of 0.23. Radical oxidation is weak during Fenton removal of the phenol-water COD.

### Effect of carrier gas

Fig.11 shows the effect of purge-gas on phenol degradation. Parameters calculated are listed in Table 5. The purge gas employed in the photo-Fenton experiments had significant impact on the COD removal. With the addition of  $\text{O}_2$  instead of  $\text{N}_2$ ,  $K_1$  increases tremendously from 0.1618 to 0.5365.  $K_1$  increases from 0.1618 to 0.3104 when air is introduced. Oxygen effect is demonstrated obviously. However, no significant increase of  $K_2$  values occurred when instead of  $\text{N}_2$ , air and  $\text{O}_2$  were introduced. The oxygen contained in air is enough for active electron transfer in the  $\text{HO}\cdot$  oxidation of phenol. From Table 5,  $K_3$  with  $\text{N}_2$  introduction is very small. This indicates that without  $\text{O}_2$  added to reaction mixture organic acid cannot be easily further oxidized.



**Fig.11 Effect of purge gas on phenol solution COD degradation**

Operational conditions:  $\text{H}_2\text{O}_2$   $Q_{\text{th}}$ ,  $\text{FeSO}_4 \cdot 7\text{H}_2\text{O}$  207 mg/L, temperature 30 °C, pH 3

**Table 5 Calculated results at different purge carrier gas**

Carrier gas	$K_1$	$K_2$	$K_3$	$K$	$\alpha$
$\text{N}_2$	0.1618	0.1147	0.0099	0.2765	1.41
Air	0.3104	0.1971	0.0280	0.5075	1.57
$\text{O}_2$	0.5365	0.2013	0.0349	0.7378	2.67

## CONCLUSION

The degradation of phenol in photo-Fenton process is different from that in UV/H<sub>2</sub>O<sub>2</sub> process. Iron complex plays an important role in this advanced oxidation process. The established model for phenol degradation is well supported by the experiment results. Operating parameters such as dosage of H<sub>2</sub>O<sub>2</sub>, ferrous ion, pH and carrier gas impact the removal of COD significantly. Under the conditions of high initial H<sub>2</sub>O<sub>2</sub> and Fe<sup>2+</sup> addition, low initial pH and dioxygen carrier gas, the calculated model parameters show that phenol is more likely degraded through complex oxidation rather than hydroxyl radical oxidation.

## References

- Andreozzi, R., Apuzzo, A.D., Marotta, R., 2000. A kinetic model for the degradation of benzothiazole by Fe<sup>3+</sup>-photo-assisted Fenton process in a completely mixed batch reactor. *J. Hazardous Materials B.*, **80**(3):241-257.
- Bossmann, S.H., Oliveros, E., Göb, S., Siegwart, S., Dahlen, E.P., Payawan, L.M., Jr, Matthias, S., Wörner, M., Braun, A.M., 1998. New evidence against hydroxyl radicals as reactive intermediates in the thermal and photochemically enhanced Fenton reactions. *J. Phys. Chem. A.*, **102**(28):5542-5550.
- Bossmann, S.H., Oliveros, E., Göb, S., Kantor, M., Goepfert, A., Braun, A. M., Lei, L., Yue, P.L., 2001. Oxidative degradation of polyvinyl alcohol by the photochemically enhanced Fenton reaction. Evidence for the formation of super-macromolecules. *Prog. React. Kinet. Mec.*, **26**(2):113-137.
- Gallard, H., Laat, J.D., 2000. Kinetic modeling of Fe(III)/H<sub>2</sub>O<sub>2</sub> oxidation reactions in dilute aqueous solution using atrazine as a model organic compound. *Wat. Res.*, **34**(12):3107-3116.
- Jiang, J., Bank, J.F., Scholes, C., 1993. Subsecond time-resolved spin trapping followed by stopped-flow EPR of Fenton reaction products. *J. Am. Chem. Soc.*, **115**(11):4742-4746.
- Kremer, M.L., Stein, G., 1959. The catalytic decomposition of hydrogen peroxide by ferric perchlorate. *Trans. Faraday Soc.*, **55**(5):959-973.
- Kremer, M.L., 1985. Complex visas 'Free Radical' mechanism for the catalytic decomposition of H<sub>2</sub>O<sub>2</sub> by Fe<sup>3+</sup>. *Int. J. Chem. Kinet.*, **17**(12):1299-1314.
- Legrini, O., Oliveros, E., Braun, A.M., 1993. Photochemical processes for water treatment. *Chem. Rev.*, **93**(2):671-698.
- Lei, L., Hu, X., Yue, P.L., Bossmann, S.H., Gob, S., Braun, A.M., 1998. Oxidative degradation of polyvinyl-alcohol by the photochemically enhanced Fenton reaction. *J. Photochem. Photobiol. A., Chem.*, **116**(3):159-166.
- Ollis, D.F., Al-Ekabi, H., 1993. Photocatalytic Purification and Treatment of Water and Air. Elsevier, Amsterdam.
- Prousek, J., 1996. Advanced oxidation processes for water treatment. Chemical processes. *Chem. Listy.*, **90**(4):229-237.
- Sun, Y., Pignatello, J.J., 1993. Photochemical reactions involved in the total mineralization of 2,4-D by Fe<sup>3+</sup>/H<sub>2</sub>O<sub>2</sub>/UV. *Environ. Sci. Technol.*, **27**(2):304-310.
- Utset, B., Garcia, J., Casado, J., Domenech, X., Peral, J., 2000. Replacement of H<sub>2</sub>O<sub>2</sub> by O<sub>2</sub> in Fenton and photo-Fenton reactions. *Chemosphere*, **41**(8):1187-1192.
- Walling, C., 1975. Fenton's reagent revisited. *Acc. Chem. Res.*, **8**(5):125-131.
- Walling, C., Amarnath, K., 1982. Oxidation of mandelic acid by Fenton's reagent. *J. Am. Chem. Soc.*, **104**(5):1185-1189.
- Weichgrebe, D., Vogelpohl, A., 1994. A comparative study of wastewater treatment by chemical wet oxidation. *Chem. Eng. Process*, **33**(4):199-203.

Welcome visiting our journal website: <http://www.zju.edu.cn/jzus>

Welcome contributions & subscription from all over the world

The editor would welcome your view or comments on any item in the journal, or related matters

Please write to: Helen Zhang, Managing Editor of JZUS

E-mail: [jzus@zju.edu.cn](mailto:jzus@zju.edu.cn) Tel/Fax: 86-571-87952276